

Neural correlates of category-specific knowledge

Alex Martin, Cheri L. Wiggs, Leslie G. Ungerleider & James V. Haxby

Laboratory of Psychology and Psychopathology, Building 10, Room 3D-41, National Institute of Mental Health, Bethesda, Maryland 20892, USA

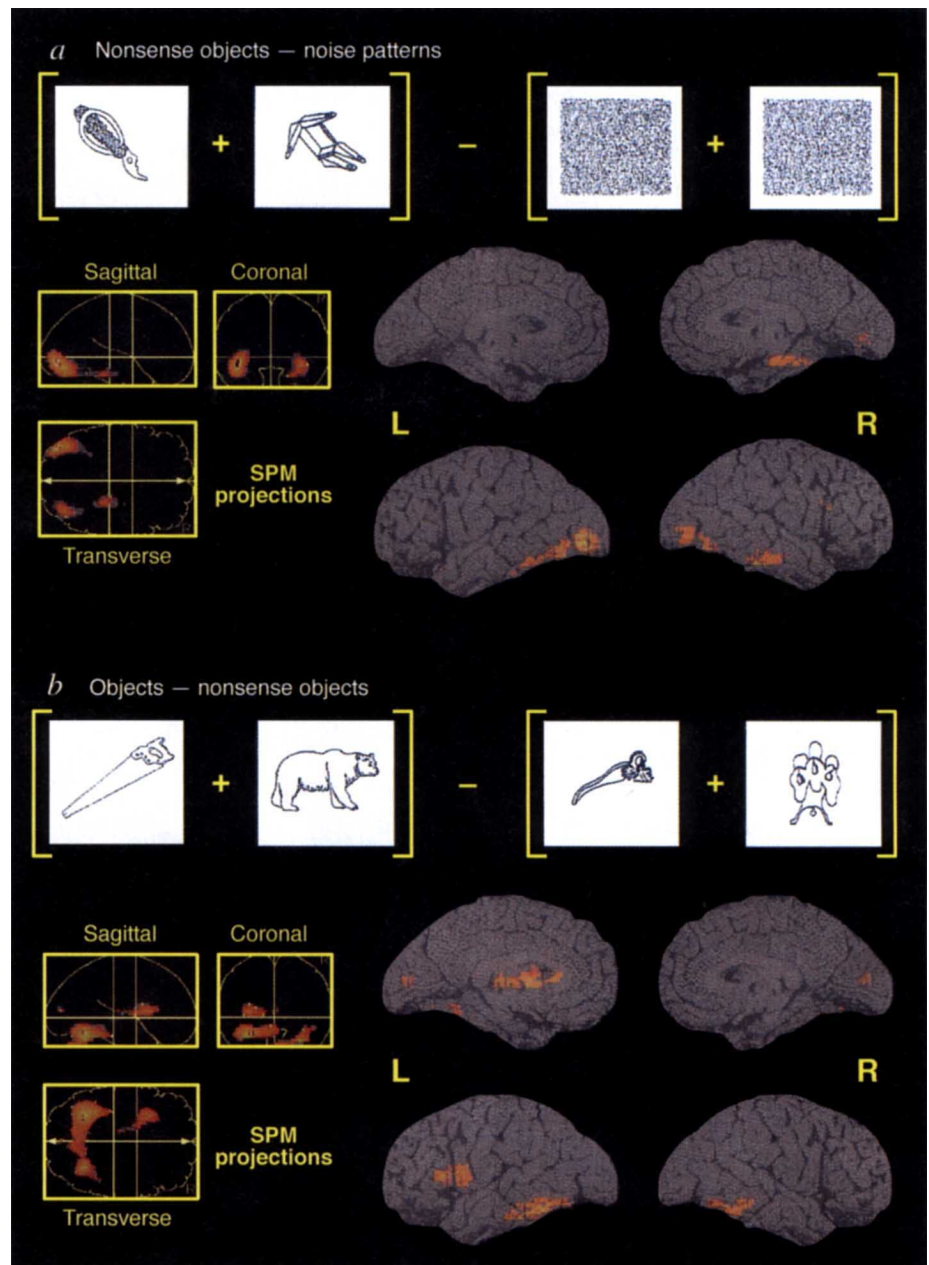
An intriguing and puzzling consequence of damage to the human brain is selective loss of knowledge about a specific category of objects. One patient may be unable to identify or name living things¹⁻³, whereas another may have selective difficulty identifying man-made objects^{4,6}. To investigate the neural correlates of this remarkable dissociation, we used positron emission tomography to map regions of the normal brain that are associated with naming animals and tools. We found that naming pictures of animals and tools was associated with bilateral activation of the

ventral temporal lobes and Broca's area. In addition, naming animals selectively activated the left medial occipital lobe—a region involved in the earliest stages of visual processing. In contrast, naming tools selectively activated a left premotor area also activated by imagined hand movements⁷, and an area in the left middle temporal gyrus also activated by the generation of action words⁸⁻¹⁰. Thus the brain regions active during object identification are dependent, in part, on the intrinsic properties of the object presented.

We studied sixteen (8 male, 8 female), right-handed subjects with positron emission tomography (PET) to measure changes in regional cerebral blood flow (rCBF) associated with identifying line drawings of animals and of tools¹¹. These categories were chosen because distinctions between four-legged animals are often based on subtle differences in physical features (form, colour and size), whereas distinctions among tools are weighted more heavily towards differences in functional attributes (how objects are used). For each category, subjects named the objects silently during one scan and out loud during another scan to provide behavioural data on naming latency and errors. To

FIG. 1 Regions of increased rCBF ($P < 0.001$) when subjects viewed nonsense objects compared to viewing visual noise patterns (a) were in the left ($-38, -82, -4$) and right ($+34, -72, -8$) inferior occipital/fusiform gyrus, the left temporal fusiform gyrus ($-26, -44, -16$), the right inferior frontal region ($+36, +16, +24$) and the left cerebellum ($-24, -36, -28$) (not shown). Activation was also present in the right parahippocampal gyrus ($+24, -32, -20; +28, -6, -28$) and right hippocampus ($+26, -16, -16$). Hippocampal activation was not found when naming real objects was compared to the visual noise baseline, suggesting that the hippocampus may be important in the detection of novelty²². Regions activated ($P < 0.001$) by naming real objects compared to viewing nonsense objects (b) were in the left ($-28, -58, -16$) and right ($+42, -44, -12$) fusiform gyri of the temporal lobes, the left anterior insula/inferior frontal region ($-28, +16, +8$), the left thalamus ($-14, -12, +8$), the calcarine sulcus ($+2, -84, +8$), and the left ($-6, -62, -16$) and right ($+4, -66, -28$) medial cerebellum (not shown). The location of activations are expressed in millimetres as coordinates in the Talairach and Tournoux brain atlas²³.

METHODS. Each stimulus was presented for 180 ms, followed by a centrally located fixation cross for 1,820 ms. Sets of animal and tool drawings were equated for name frequency and category typicality. Different sets were presented during the silent and overt naming conditions, counterbalanced across subjects. PET scans were obtained using a Scanditronix PC2048-15B tomograph (Milwaukee, Wisconsin) which acquires 15 continuous, 6.5-mm-thick cross-sectional images. Within-plane resolution is 6.5 mm (full width at half maximum). Subjects began the task ~30 s before injection of 37.5 mCi of $H_2^{15}O$. Data were analysed using Statistical Parametric Mapping (SPM)²⁴⁻²⁶. Data from each subject were normalized to his/her own global mean flow (ratio correction). Contrasts between tasks were evaluated with *t*-tests, and then converted to *z* scores.



investigate further the object-processing system and to establish baselines for comparison purposes, subjects were also scanned twice while staring at visual noise patterns, and twice while staring at novel nonsense objects¹². The data are shown from the six PET scans during which there was no overt speech (Fig. 1).

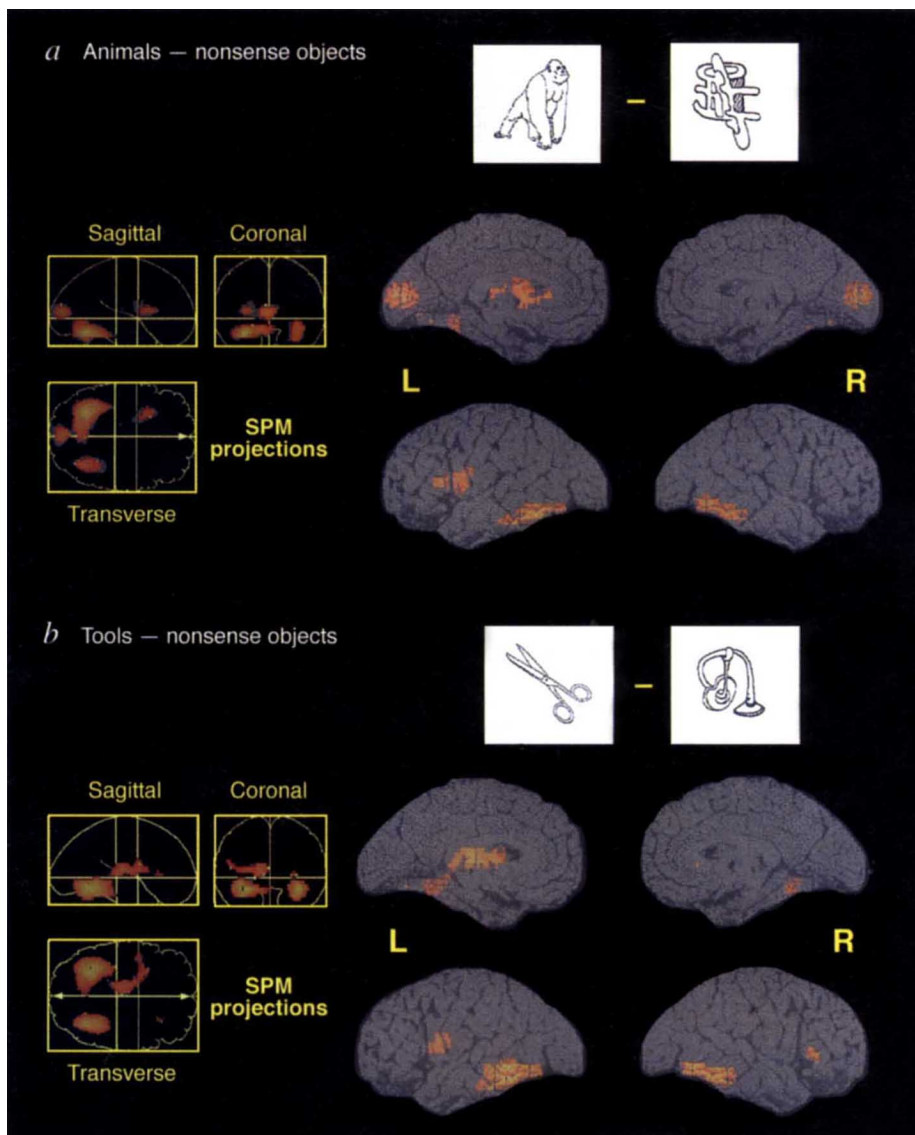
Activation of a hierarchically organized, ventral occipitotemporal object processing stream¹³ was revealed by first comparing perception of noise patterns to nonsense objects (Fig. 1a), and then comparing perception of nonsense objects to silent object naming (animal and tool conditions combined) (Fig. 1b). Relative to perceiving visual noise, perceiving nonsense objects activated the left and right fusiform and inferior gyri of the occipital lobes (Brodmann's area (BA) 19). Relative to viewing nonsense objects, naming real objects also produced bilateral ventral activation that coincided with, and extended anterior to, the activation produced by viewing nonsense patterns. Thus, relative to viewing nonsense objects, the ventral temporal lobes showed increased activity during object naming, whereas the inferior occipital regions did not. Increased rCBF during object naming was also seen in the left insula/Broca's area, as reported in other PET studies of silent word generation⁸ (see figure legends for complete listing of activations).

Identifying real objects also activated the calcarine sulcus (BA 17), or primary visual cortex (Fig. 1b), but calcarine activation occurred only for naming animals (Fig. 2). In addition, although identifying animals and tools were both associated with bilateral

increases in rCBF in the ventral region of the temporal lobes, the left temporal activation extended dorsally to include the middle temporal gyrus for naming tools, but not animals (Fig. 2). Finally, naming tools, but not animals, was associated with activation of the left premotor area (BA 4/6). These category-specific rCBF differences were also observed when the animal and tool conditions were directly contrasted with each other, thus providing strong evidence that rCBF, and hence neuronal activity, was modulated by the type of object presented. Relative to naming tools, naming animals produced a large area of activation in the left medial occipital lobe centred on the calcarine sulcus (Fig. 3), whereas, relative to naming animals, tool-naming produced activity in the left middle temporal gyrus (BA 21) and the left premotor region (BA 6).

Selective activation of the medial aspect of the occipital lobe during animal naming suggests that these stimuli placed greater demands on early stages of visual processing. Indeed, the animal pictures triggered a slower and less accurate response than the tools. However, increased early visual processing demands could not alone account for this finding. The viewing conditions for each task were identical, yet the medial occipital region was activated when naming animals, but not when naming tools, nor when viewing visually complex nonsense objects. To rule out the effects of stimulus complexity, a different group of subjects ($n = 16$) were investigated under the same conditions as in the first study except that objects were presented in silhouette, thereby eliminating

FIG. 2 Regions of increased rCBF ($P < 0.001$) when subjects silently named drawings of animals compared to viewing nonsense objects (a) were in the calcarine sulcus ($-2, -82, +8$), the left ($-24, -58, -16$) and right ($+34, -56, -12$) fusiform gyri of the temporal lobes, the left putamen ($-20, +4, +8$), left thalamus ($-18, -10, +16$), left insula/inferior frontal region ($-28, +14, +8$), and the right lateral ($+32, -60, -20$) and medial ($+8, -56, -28$) cerebellum (not shown). Regions of increased rCBF ($P < 0.001$) when subjects silently named tools compared to viewing nonsense objects (b) were the left ($-28, -50, -12$) and right ($+34, -50, -12$) fusiform gyri of the temporal lobes, left inferior temporal gyrus ($-36, -48, -4$), left putamen ($-24, +4, +8$), left thalamus ($-12, -18, +8$), left insula/inferior frontal region ($-30, +8, +8$), left precentral gyrus (BA 4/6) ($-36, 0, +12$), right inferior frontal gyrus (BA 45) ($+28, +28, +4$), and the right medial cerebellum ($+8, -56, -28$) (not shown). The animal pictures have been judged to be more visually complex and less familiar than the tools¹¹. Consistent with these differences, behavioural data recorded during the overt-naming PET scans indicated that the animal pictures were named more slowly and less accurately than were the tools ($P < 0.01$) (the mean \pm standard error of the mean for voice response time was 620 ± 21.2 ms and error rate was $16.7 \pm 0.77\%$ for naming animals; mean \pm standard error was 566 ± 21.0 ms and the error rate was $10.0 \pm 0.54\%$ for naming tools).



internal detail. This manipulation ruled out differences between the animal and tool stimuli in naming latency and naming errors. Nevertheless, relative to naming tool silhouettes, naming animal silhouettes activated the left medial occipital area (Fig. 3 legend). Selective activation of the occipital cortex during animal naming may reflect top-down modulation, or reactivation, of primary visual areas, rather than increased visual processing during input¹⁴⁻¹⁶. Reactivation of this region may be necessary to identify an object uniquely when relatively subtle differences in physical features are the primary means by which the object can be distinguished from other members of its category.

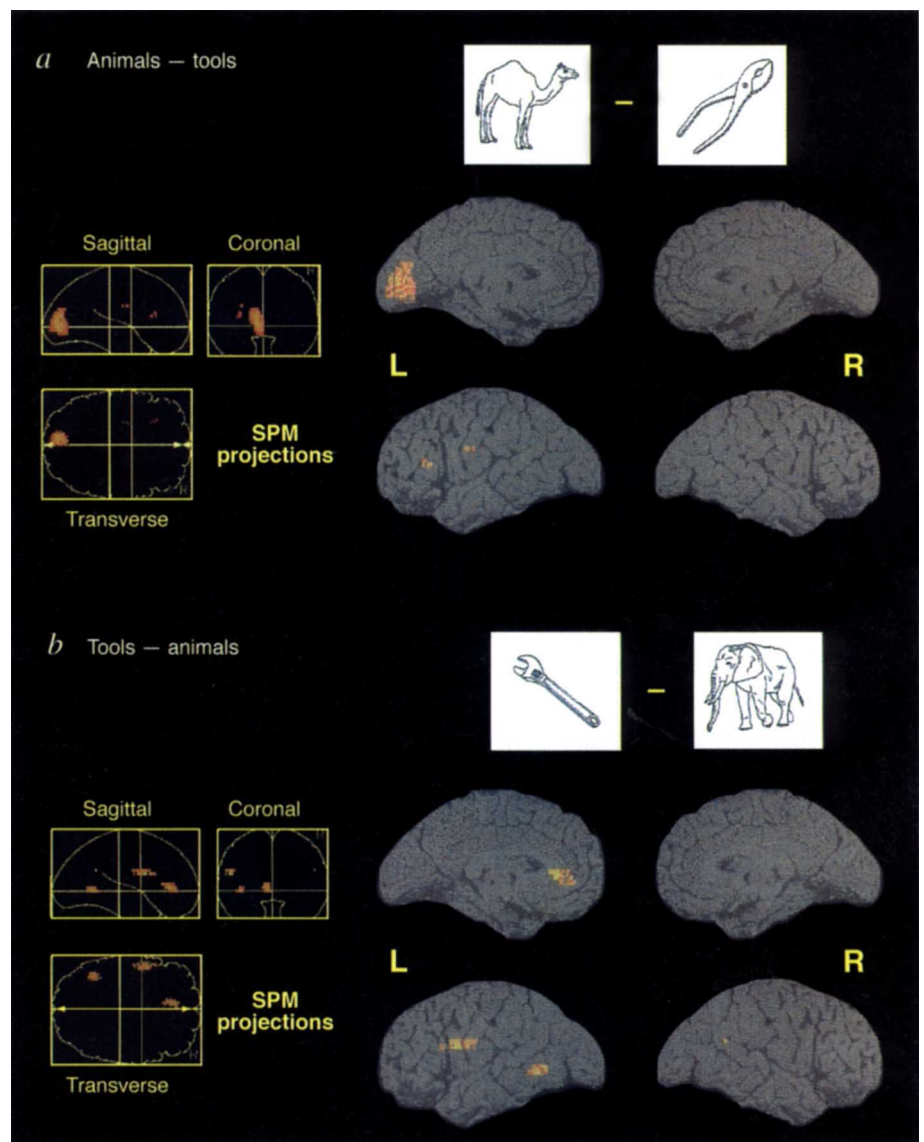
The region of the left middle temporal gyrus active when identifying tools, but not animals, was nearly identical to the area activated in previous studies in which subjects generated action words associated with objects⁸⁻¹⁰. Thus, this region, which lies just anterior to the area active when perceiving movement^{17,18}, may be the site for stored knowledge about patterns of visual motion associated with using objects. The region of the left premotor cortex activated when subjects named tools, but not animals, was nearly identical to the area activated when subjects

imagined grasping objects with their right hand⁷. This premotor area, therefore, may be the site for stored knowledge about how objects are used. Both the left middle temporal gyrus and the left premotor cortex were also selectively activated by naming tool silhouettes relative to naming animal silhouettes (Fig. 3 legend). Thus, identifying tools may be mediated, in part, by areas that mediate knowledge of object motion, and of object use. Moreover, these representations appear to be stored close to the tissue that is active when perceiving motion and when using objects¹⁰.

Although patients with category-specific deficits typically have large lesions, difficulty naming living things has been associated with posterior and ventral lesions, whereas selective difficulty naming man-made objects has been associated with lesions that are anterior and dorsal¹⁹. Our findings are in agreement with this broad anatomical distinction but still provide a level of detail not previously available from studies on brain-damaged patients.

We have the capacity to identify a tremendous number of objects quickly and accurately. This ability is dependent, in part, on the automatic activation of previously acquired knowledge about the physical and functional attributes that define these

FIG. 3 Regions of increased rCBF when subjects silently named drawings of animals compared to silently naming tools (a), and when they silently named tools compared to silently naming animals (b). The strength of these activations were not as great as when each naming condition was compared to the nonsense object baseline condition (Fig. 2). To illustrate the spatial extent of these activations the threshold was set at $Z > 2.32$ ($P < 0.01$, 1-tailed), whereas the threshold for the activations depicted in Figs 1 and 2 was set at $Z > 3.09$, ($P < 0.001$, 1-tailed). Regions activated by animal naming compared to tool naming (a) were in the calcarine sulcus ($-4, -80, +8$; $Z = 3.12$). There were also two small activations in the left frontal lobe ($-26, -6, +24$; $Z = 2.50$, and $-26, +28, +16$; $Z = 2.41$). Regions activated by tool naming compared to animal naming (b) were in the left middle temporal gyrus ($-36, -50, +4$; $Z = 2.90$), left anterior cingulate (BA 32) ($-6, -38, +2$; $Z = 2.78$), right supramarginal gyrus ($+48, -50, +24$; $Z = 2.50$), and left lateral inferior frontal cortex, extending from BA 44 ($-52, +10, +20$; $Z = 2.85$) to premotor cortex (BA 6) ($-48, 0, +20$; $Z = 2.74$). Silhouette study: The voice response time was 703 ± 31.0 ms and error rate was $17.2 \pm 3.01\%$ for naming silhouettes of animals. The voice response time was 679 ± 24.4 ms and error rate was $15.6 \pm 4.05\%$ for naming tool silhouettes ($P > 0.10$). A region-of-interest analysis was applied to the rCBF data based on all pixels that exceeded a threshold of $Z = 2.32$ ($P < 0.01$) from the first study. Analysis of these regions indicated that, relative to naming silhouettes of tools, naming animal silhouettes activated the left medial occipital region ($F(1, 15) = 3.96$, $P < 0.05$) with maximal peak activity at $-18, -90, +12$ ($Z = 2.86$) and $-2, -84, -4$ ($Z = 2.63$), whereas, relative to naming animal silhouettes, tool silhouette naming activated the left middle temporal region ($F(1, 15) = 4.29$, $P < 0.05$) with maximal peak activity at $-40, -62, +4$ ($Z = 3.51$), and the left premotor region ($F(1, 15) = 8.43$, $P < 0.005$) with maximal peak activity at $-42, 0, +20$; $Z = 2.59$).



objects^{20,21}. Our results suggest that semantic representations of objects are stored as a distributed neural network that includes the ventral region of the temporal lobe. The location of the other areas recruited as part of this network depends on the intrinsic properties of the object to be identified. □

Received 11 July; accepted 1 December 1995.

1. Warrington, E. K. & Shallice, T. *Brain* **107**, 829–854 (1984).
2. Silveri, M. C. & Gainotti, G. *Cog. Neuropsychol.* **5**, 677–709 (1988).
3. Sheridan, J. & Humphreys, G. W. *Cog. Neuropsychol.* **10**, 143–184 (1993).
4. Warrington, E. K. & McCarthy, R. *Brain* **106**, 859–878 (1983).
5. Warrington, E. K. & McCarthy, R. *Brain* **110**, 1273–1296 (1987).
6. Sacchetti, C. & Humphreys, G. W. *Cog. Neuropsychol.* **9**, 73–86 (1992).
7. Decety, J. et al. *Nature* **371**, 600–602 (1994).
8. Wise, R. et al. *Brain* **114**, 1803–1817 (1991).
9. Raichle, M. E. et al. *Cereb. Cortex* **4**, 8–26 (1994).
10. Martin, A. et al. *Science* **270**, 102–105 (1995).
11. Snodgrass, J. G. & Vanderwart, M. J. *exp. Psychol.: Hum. Learn. Mem.* **6**, 174–215 (1980).
12. Kroll, J. F. & Potter, M. C. *J. verb. Learn. verb. Behav.* **23**, 39–66 (1984).
13. Ungerleider, L. G. & Mishkin, M. in *Analysis of Visual Behavior* (eds Ingle, D. J., Goodale, M. A. & Mansfield, R. J. W.) 549–586 (MIT Press, Cambridge, MA, 1982).
14. Damasio, A. R. *Cognition* **33**, 25–62 (1989).
15. Farah, M. J. *Trends Neurosci.* **12**, 395–399 (1989).
16. Kosslyn, S. M. et al. *J. Cogn. Neurosci.* **5**, 263–287 (1993).
17. Corbetta, M., Miezin, F. M., Dobmeyer, S., Shulman, G. L. & Petersen, S. *Science* **248**, 1556–1559 (1990).
18. Zeki, S. et al. *J. Neurosci.* **11**, 641–649 (1991).
19. Saffran, E. M. & Schwartz, M. F. in *Attention and Performance XV* (eds Umiltà, C. & Moscovitch, M.) 507–536 (MIT Press, MA, 1994).
20. Glaser, W. R. *Cognition* **42**, 61–105 (1992).
21. Humphreys, G. W., Riddoch, M. J. & Quinlan, P. T. *Cog. Neuropsychol.* **5**, 67–103 (1988).
22. Tulving, E., Markowitsch, Kapur, S., Habib, R. & Houle, S. *NeuroReport* **5**, 2525–2528 (1994).
23. Talairach, J. & Tournoux, P. *Co-planar Stereotaxic Atlas of the Human Brain* (Thieme, New York, 1988).
24. Friston, K. J. et al. *J. cereb. Blood Flow Metab.* **10**, 458–466 (1990).
25. Friston, K. J. et al. *J. cereb. Blood Flow Metab.* **9**, 690–699 (1991).
26. Friston, K. J., Frith, C. D., Liddle, P. F. & Frackowiack, R. S. J. *J. comput. assist. Tomogr.* **15**, 634–639 (1991).

Creation of a biologically active interleukin-5 monomer

Richard R. Dickason & David P. Huston

Baylor College of Medicine, Departments of Medicine, and Microbiology and Immunology, One Baylor Plaza, FBRN B567, Houston, Texas 77030, USA

INTERLEUKIN-5 (IL-5) specifically induces the differentiation of eosinophils, which are important in host defence and the pathogenesis of allergies and asthma^{1,2}. Structurally, IL-5 is a unique member of the short-chain helical-bundle subfamily of cytokines whose canonical motif contains four helices (A–D) arranged in an up–up–down–down topology^{3,4}. In contrast to other subfamily members, which fold unimolecularly into a single helical bundle^{5–8}, IL-5 forms a pair of helical bundles by the interdigitation of two identical monomers that contribute a D helix to the other's A–C helices³. We predicted that the lack of bioactivity by an IL-5 monomer⁹ was due to a short loop between helices C and D which physically prevents unimolecular folding of helix D into a functionally obligate structural motif. Here we report that, by lengthening this loop, we have engineered an insertional mutant of IL-5 that was expressed as a monomer with biological activity similar to that of native IL-5. These studies demonstrate that all of the structural features necessary for IL-5 to function are contained within a single helical bundle.

The consensus motif of helical-bundle cytokines requires the connection of helices A and B and helices C and D by long overhand loops (loops 1 and 3), and the connection of helices B and C by a short turn (loop 2)⁴. To determine the structural element(s) of interleukin-5 (IL-5) that influence its unique interdigitating homodimeric configuration, we compared the primary sequences of the secondary structural elements within IL-5 with the four other short-chain helical-bundle cytokines, these being IL-2, IL-4, granulocyte–macrophage–colony-stimulating factor

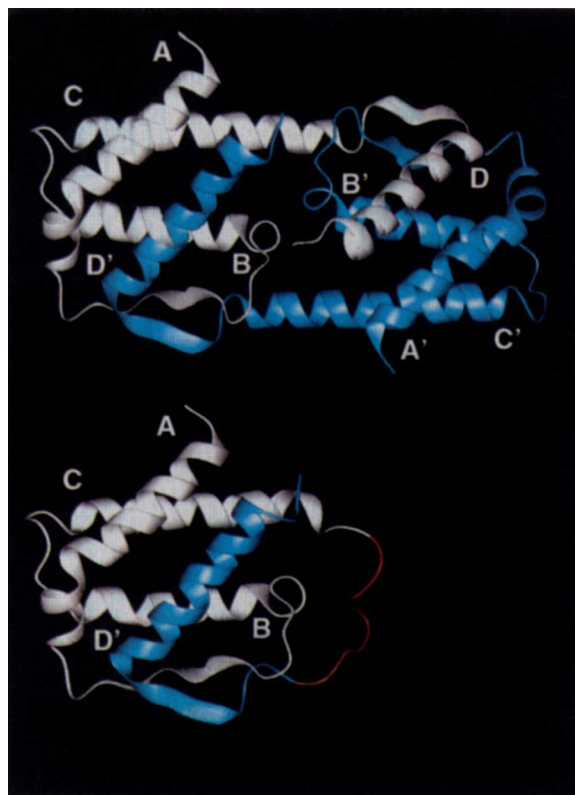


FIG. 1 Modelling of mono5. The top ribbon diagram represents the IL-5 interdigitating homodimer in which one monomer, with helices labelled A–D, is white and the other monomer, with helices labelled A'–D', is blue. Letters are located at the N-terminal end of each helix. The bottom ribbon diagram represents the modelled structure of mono5. This composite structure consists of residues 1–84 of one IL-5 monomer (white), residues 85–115 of the other IL-5 monomer (blue), and an insert (red) from residues 87–94 of the analogous loop 3 region of GM-CSF (His-Cys-Pro-Thr-Pro-Glu-Thr). This GM-CSF sequence contained three prolines, which favoured the extended secondary structure required to span the existing gap and did not perturb the helical-bundle conformation. To avoid aberrant formation of disulphide bonds, the cysteine at position 2 of the GM-CSF residues was changed to serine. The sequence for mono5 was constructed by replacing the *EaeI* and *BspMI* fragment of a previously reported human IL-5 construct¹¹ with a synthetic double-stranded insert. The insert encoded the native IL-5 sequence between the *EaeI* and *BspMI* sites, in addition to the eight codons of the modified GM-CSF loop 3 sequence. These eight codons were positioned between the native IL-5 codons for Lys 84 and Lys 85. Structural analysis of the short-chain helical-bundle cytokines used coordinates deposited in the Brookhaven Protein Databank (IL-2, 3ink⁵; IL-4, 1rcb⁶; GM-CSF, 1gmf⁷; and M-CSF, 1hmc⁸). The IL-5 coordinates were provided by S. Jordan³. The structures were displayed, manipulated and minimized on a Silicon Graphics workstation using the QUANTA software package (Keck Center for Computational Biology).

(GM-CSF), and M-CSF^{3,5–8}. IL-5 was distinguished by a shorter loop 3, containing only eight amino acids, which differed significantly from the 15–20 residues for the other short-chain helical-bundle cytokines. We therefore considered that the length of loop 3 might determine whether a helical-bundle cytokine will be actively expressed as a monomer or as an interdigitating homodimer. Molecular modelling suggested that lengthening loop 3 of IL-5 by eight amino acids would relieve the intramolecular folding constraint and enable unimolecular formation of a complete, and potentially functional, helical bundle.

A computer-generated image of the tertiary structure of IL-5 was modified by deletion of residues C-terminal to Lys 84 of one monomer, and residues N-terminal to Lys 85 of the other monomer. This targeted a site for insertional mutagenesis that preserved the stabilizing interhelical interactions, the β -strand